J. Micromech. Microeng. **19** (2009) 055009 (10pp) doi:10.1088/0960-1317/19/5/055009

A reusable micromechanical energy storage/quick release system with assembled elastomers

Sarah Bergbreiter[1,4], **Deepa Mahajan**[2] **and Kristofer S J Pister**[3]

[1] Department of Mechanical Engineering, University of Maryland, 2181 Glenn L. Martin Hall, College Park, MD 20742, USA
[2] Department of Electrical Engineering, Stanford University, 161 Packard Building, 350 Serra Mall, Stanford, CA 94305, USA
[3] Berkeley Sensor and Actuator Center, UC Berkeley, 497 Cory Hall, Berkeley, CA 94720, USA

E-mail: sarahb@umd.edu

Received 20 December 2008, in final form 8 March 2009
Published 15 April 2009
Online at stacks.iop.org/JMM/19/055009

Abstract
A reusable, elastomer-based energy storage/quick release system for MEMS has been designed, built and tested. Microrubber bands have been fabricated from silicone using two different methods, laser cut and molded, and assembled into silicon microstructures fabricated in a two-mask silicon-on-insulator (SOI) process. Using silicon hooks and force gauges designed in this process, these microrubber bands have been characterized as to their energy storage potential and efficiency by stretching them with a probe tip. These tests showed recovered energy efficiencies up to 92% at strains over 200% with a maximum stored energy over 19 μJ. In addition, a fully integrated micromechanical energy storage system to both store and release energy has been demonstrated using an electrostatic inchworm motor to stretch the elastomer band and release it. Using the inchworm motor, an estimated 4.9 nJ of energy was stored in the elastomer spring and quickly released.

(Some figures in this article are in colour only in the electronic version)

1. Introduction

The goal of this project is to build a reusable mechanical energy storage system for eventual use in an autonomous jumping microrobot. Like a flea, a millimeter-sized microrobot requires a micromechanical energy storage system to store energy and release it quickly to jump. Autonomous microrobots have the potential for use in mobile sensor networks, search and rescue and micro-construction tasks [1]. In addition to jumping microrobots, the energy storage system demonstrated in this paper could be used in any MEMS system requiring a large release of energy in a short period of time [2–4].

Despite the utility of such a system and its prevalence in biology and the macroworld, very few examples of mechanical energy storage systems have been found in MEMS. Rogers *et al* used comb drive actuators and a set of gears to store energy in silicon springs [3]. A fuse was blown to release energy in a single shot rendering the device inadequate for reuse. Elastomer springs are ubiquitous for mechanical energy storage at the macroscale and their material properties, particularly low Young's modulus and high strains, have made elastomer an attractive material for use in MEMS systems as well. In [5], polydimethylsiloxane (PDMS) springs were used to attach a proof mass to fixed capacitor plates in an accelerometer. PDMS was also used to create flexural joints in [6] to convert in-plane to out-of-plane motion. Both of these applications integrated the elastomer with silicon by using relatively complex fabrication processes. In [5], the silicone used was a special PDMS patterned by UV light and [6] required specialized bonding equipment and alignment with previously fabricated silicon structures.

In this paper, a reusable micromechanical energy storage system will be composed of a spring, a low power actuator to store energy in the spring, and a clamping system to

[4] All work carried out at the Berkeley Sensor and Actuator Center at UC Berkeley.

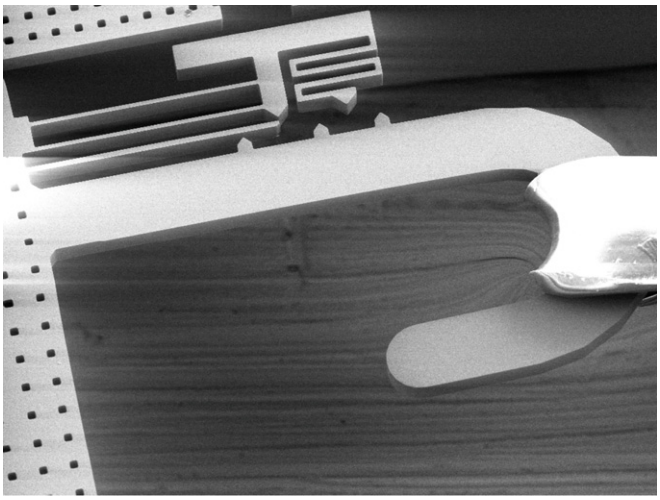

Figure 1. Silicon hook fabricated in an SOI wafer with microrubber band attached.

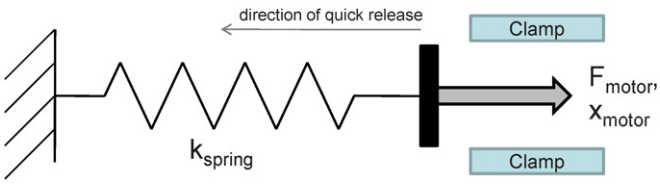

Figure 2. Model of reusable micromechanical energy storage/quick release system.

release the energy quickly (figure 2). Low input power to the actuators will be important for the small, low power devices that this system will enhance. Quick release of the energy is also important to provide the mechanical power amplification needed for a robot to jump. In an ideal world, the system would require no mass or volume, be 100% efficient at transferring stored strain energy to released energy, be simple to fabricate with low power actuators and would perfectly match the force/displacement characteristics of the low power actuators chosen.

The following sections outline the design decisions that led to choosing an assembled elastomer spring, along with a process in which elastomer springs are fabricated separately and later assembled into silicon microstructures. This technique not only simplifies the fabrication process, but also allows the use of elastomers not compatible with previously demonstrated processes. The fabricated elastomers are then characterized and demonstrated in a fully integrated micromechanical energy storage/quick release system.

2. Design

A number of factors should be considered while designing and fabricating a micromechanical energy storage system, and a number of tradeoffs exist in the design space. The primary application for this system is power amplification through the quick release of energy, with the goal of reaching over 1 mW mg^{-1} in a jumping microrobot as seen in jumping insects [7]. The spring in figure 2 will therefore require high energy storage density, low loss during a quick release and a fabrication process that can easily be integrated with power efficient MEMS motors. This section examines different spring materials to weigh the tradeoffs of spring energy density, efficiency, fabrication and integration. For example, silicon springs may be simple to fabricate and integrate with certain MEMS actuators as shown in [3], but they will require a large area and very high forces.

2.1. Energy density

One of the simplest ways to store mechanical strain energy is through tension as done in rubber bands and tendons. The maximum energy that can be stored in a beam of length L and cross-sectional area A under tension is described by $U_{\max}$, where τ is the material yield strength, E is the Young's modulus and $\epsilon_{\max}$ is the maximum elastic strain supported by the material

$$U_{\max} = \frac{1}{2} F_{\max} x_{\max} = \frac{1}{2} \frac{Al\tau^2}{E} = \frac{1}{2} AlE\epsilon_{\max}^2. \quad (1)$$

The energy stored in a given mass is provided by the following equation where ρ is the material density:

$$\frac{U_{\max}}{Mass} = \frac{1}{2\rho} \frac{\tau^2}{E} = \frac{1}{2\rho} E\epsilon_{\max}^2. \quad (2)$$

Relevant material properties are given in table 1. Resilin and locust apodeme (cuticle) are both materials used as springs in insects. Resilin is a soft, rubbery material used in shear and compression for very small insects like fleas, and cuticle is a stiffer material used in bending modes in somewhat larger insects like locusts. Silicon, polydimethylsiloxane (PDMS or silicone), parylene, polyimide and polyurethane are provided as examples of materials seen in microfabrication and range from stiff and brittle silicon to soft and flexible PDMS. As seen in this table, the practical strain limit of silicon reduces its energy storage density to over two orders of magnitude below polyurethane and an order of magnitude below PDMS. Stiffer materials also have a number of tradeoffs including the high force or high mechanical advantage required by the actuators.

2.2. Spring efficiency

In an energy storage and rapid release system, spring efficiency will ultimately relate the amount of energy released by the system to the amount of potential energy originally stored in the spring. The spring material will affect efficiency through energy losses due to heat or other mechanisms that occur while stretching the material.

All of the materials above experience some amount of energy loss as they stretch. In polymers, the long, convoluted molecular chains composing the polymers are straightened when the material is stretched, losing some amount of energy to friction and heat. In a material like silicon, very little energy is lost due to the rigid crystalline nature of the material. Polymers are somewhat more complex and energy loss can be characterized by the dissipation factor, $\tan(\delta)$ where δ is the ratio between the complex modulus which determines

Table 1. Possible spring material characteristics.

Material	E (GPa)	τ (MPa)	Energy/volume (mJ mm^{-3})	Energy/mass (mJ mg^{-1})
Silicon [8]	190	500	0.66	0.28
PDMS [9, 5]	0.000 75	2.2	3.3	3.4
Parylene [10]	3.2	55	0.5	0.4
Polyimide [11]	3.3	64.3	0.6	0.4
Polyurethane [12]	0.0076	38	95	76
Resilin [7]	0.002	3	2.25	2.1
Locust apodeme [7]	20	600	9	7.5

Table 2. Fabrication complexity for spring materials and designs.

Materials	
Silicon	Easy
PDMS [6]	Medium/difficult
Parylene [15]	Medium
Polyimide [11]	Medium/difficult
Polyurethane [16]	Medium/difficult

Table 3. Spring sizes for different materials in tension.

Material	Length (mm)	Area (μm^2)
Silicon	1900	20
Resilin	3.3	3300
Locust apodeme	170	17
PDMS	1.7	4500
Parylene	290	180
Polyimide	260	160
Polyurethane	1	260

viscosity and the real modulus which governs elasticity. A higher dissipation factor indicates a more viscous material more likely to lose energy when stretched [13]. For example, polyurethane, which has a dissipation factor of 0.14–100 Hz, will demonstrate a greater hysteresis than PDMS which has a dissipation factor closer to 0.001 [12]. PDMS and materials with a similarly low dissipation factor will remain a highly efficient spring material and will allow most of the energy stored in the spring to be delivered upon release.

2.3. Spring fabrication and integration

The practicality of the materials and spring designs discussed thus far will depend heavily on fabrication capabilities, and the difficulty in fabricating these springs will be primarily governed by integration with the actuators. While it is not simple to quantify these challenges, it is assumed that the low power actuator used to store energy in the system will be fabricated in a silicon MEMS-based process like the motors in [14], and previous work is used to evaluate some measure of compatibility with this process. Table 2 provides relative measures of fabrication simplicity for the materials discussed above.

Given that the actuators are fabricated in a silicon MEMS process, silicon springs may in fact be the simplest to fabricate with silicon motors as was seen in [3]. Recent work by Suzuki and Tai has shown parylene springs integrated with silicon parts for use in inertial sensors although this adds an extra mask step to the fabrication process [15]. Mahadevon used polyimide for springs to measure the work done by microactuators in [11]. Currently, the most common polymer used in MEMS is PDMS although it is generally used with soft lithography to build microfluidic devices at large scales. However, Tung and Kurabayashi used PDMS as a spring material with silicon actuators, albeit with a relatively complex fabrication process [6]. Finally, polyurethane has been integrated with silicon MEMS to create artificial hair cell sensors in [16].

Fabrication, however, may be simplified in a number of ways. The post-process assembly of simple silicon parts in a one-mask process was recently demonstrated by Last in [17] and similar ideas may be translated to the fabrication of an energy storage system. Materials like PDMS which have not been fabricated with silicon structures in the past may instead be assembled post-process which removes the need for more complex bonding and alignment steps in the clean room. For a spring in tension, this may be as simple as assembling a very tiny rubber band.

Not only does the energy storage system need to be attached to the motors, it should also match the characteristics of those motors. The material properties listed in table 1 provide data to calculate the forces and displacements that the material can support if designed as a beam placed in tension. Table 3 lists the dimensions required for a beam in tension to support the force/displacement characteristics reasonable for the actuators in [14] (10 mN and 5 mm, respectively). While the stiffer materials would generally be used in bending instead of tension, this table provides a rough idea of the compatibility of these spring materials with the actuators. For example, a PDMS spring requires a length of 1.7 mm and a cross-sectional area of 45 $\times$ 100 μm^2 to support these forces and displacements, and a spring with these dimensions would be straightforward to fabricate and fit into a millimeter-sized microsystem. On the other hand, a silicon spring would require a length of 1.9 m and a cross-sectional area of 4 $\times$ 5 μm^2—a significantly greater challenge for fabrication and integration into a system of this size.

In the end, it was determined that a linear elastomer spring offered the greatest number of benefits and least number of drawbacks in fabricating a reusable micromechanical energy storage system. PDMS is small, lightweight, efficient and matches the actuators described in [14] very well. The fabrication drawback of integrating PDMS with silicon actuators will be solved by using a post-process assembly

technique described in the following section. One of the simplest examples of a linear elastomer spring is the rubber band. The following few sections will discuss the fabrication and characterization of microrubber bands for a reusable micromechanical energy storage system.

3. Fabrication

In order to simplify the fabrication process for this elastomer-based micromechanical energy storage system, two separate processes are used and the final structures are assembled together. A simple two-mask silicon process is used to build high force motors, attachment hooks and test structures to characterize the elastomers. To fabricate the microrubber bands, both a laser cutting method and molding process are demonstrated and compared.

3.1. Silicon fabrication

The primary goals of the silicon fabrication process are to build actuators capable of storing energy in the microrubber bands and build attachment points for connecting the elastomer to those actuators. The actuators must be capable of high forces combined with large displacements to store large amounts of energy while consuming low power. Finally, attachment to those actuators must be provided so that microrubber bands may be assembled without difficulty.

For the actuators, electrostatic inchworm motors [14] were chosen due to their compatibility with the requirements listed above. Inchworm motors use gap closing actuators (GCAs) and accumulate the resulting displacements to create the possibility of unlimited travel. While inchworm motors may be fabricated in a single mask silicon-on-insulator (SOI) process, the attachment points for assembling the microrubber bands into the inchworm motors require a backside etch to leave room for the rubber bands to extend through the wafer. Hooks (figure 1) were chosen as attachment points and are fabricated in the top layer of an SOI wafer.

The final result is a simple two-mask process that etches both sides of an SOI wafer (figure 3). The process starts on a 4 inch SOI wafer with a 20 μm structure layer (frontside), 2 μm buried oxide (BOX) and 300 μm substrate (backside). The front is patterned first and etched using a surface technology systems (STS) advanced silicon etch. The exposed buried oxide is removed using an RIE oxide etcher and the front is protected by depositing 0.6 μm of low temperature oxide (LTO). The backside is aligned and patterned using a Karl Suss contact printer with backside alignment. Another STS advanced silicon etch is used to etch through the backside, terminating on the BOX layer or LTO deposited earlier. Finally, the structures are released using a timed 49% HF wet etch and a critical point dry.

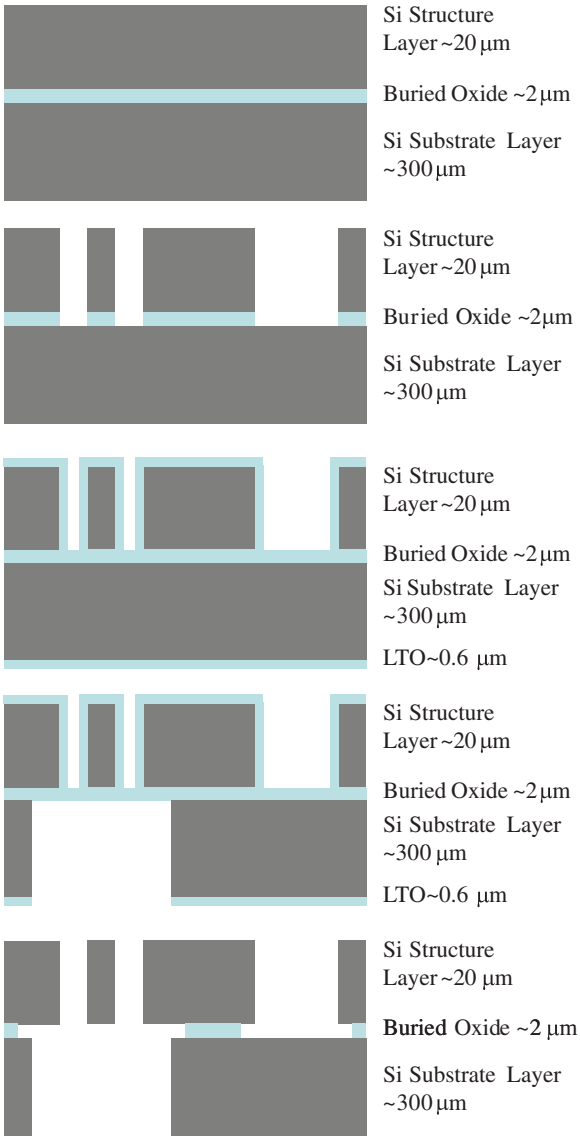

Figure 3. A two-mask SOI process with front and back etches to build motors and hooks.

3.2. Elastomer fabrication

Two different processes are used to fabricate the elastomer springs and are distinguished by the method in which the elastomer is patterned. The first method cuts the elastomer using a laser and the second uses a silicon mold to define the spring shape. Both of these methods currently use Dow Corning Sylgard® 186 silicone for the elastomer. Sylgard® 186 was chosen due to its high tear strength and high strains previously characterized in [18]. However, Sylgard® 186 also has a relatively high viscosity of 65 000 cps making it difficult to work with. To thin the Sylgard® 186, it is mixed with Dow Corning 200® Fluid (50 cst) at a ratio of 10:1 by weight. In addition, before using in either fabrication method, the mixture is placed in vacuum at approximately 1 torr for 30 min to reduce the number of bubbles and produce a higher quality cured silicone.

3.2.1. Laser cutting. The first method, laser cutting, does not require the use of a clean room and provides a fast turnaround time. Thinned Sylgard® 186 is spun onto a silicon wafer to a thickness of approximately 50 μm by slowly ramping the spinner speed to 3500 rpm and holding it there

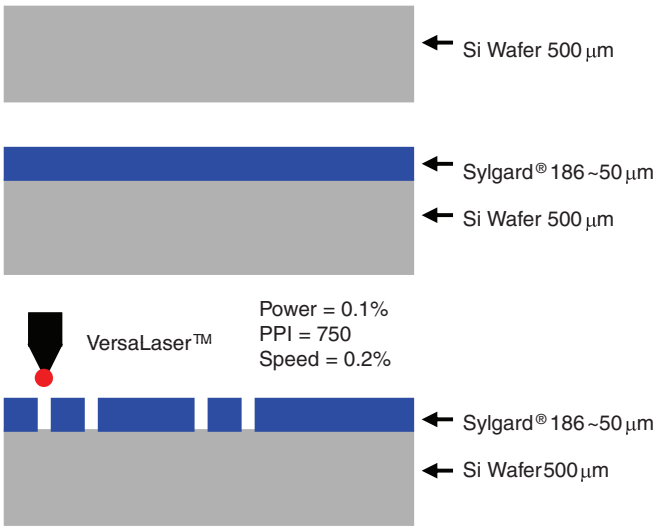

Figure 4. Process for laser cutting microrubber bands.

for 60 s. After curing the silicone at 100 °C for 45 min, a VersaLaser® IR commercial laser cutting tool is used to cut the elastomer into given patterns. Patterns are designed as a SolidWorks® drawing and are printed onto the silicone using the VersaLaser® print driver where power, pulses per inch (PPI) and speed are all definable options. The best settings found thus far for cutting Sylgard® 186 are power = 0.1%, PPI = 750 and speed = 0.2%. Percentages are defined relative to unknown maximum values internal to the VersaLaser™. The process flow is shown in figure 4.

While the laser cutting process is quick and easy, it is not perfect. The cuts provided by the laser result in jagged edges, and the positional resolution is on the edge of 'good enough' to cut out 75 μm wide rubber bands (figure 5). In fact yield is generally only 10–20% due to errant cuts that slice through the rubber band. In addition, patterning anything other than bands can be difficult with the VersaLaser® due to these same errant cuts.

3.2.2. Molding. Molding provides higher quality rubber bands, higher yield and more flexibility in spring design. In this method (figure 6), silicon molds are fabricated by patterning and etching a silicon wafer using the STS advanced silicon etch. The molds are then passivated, using a process

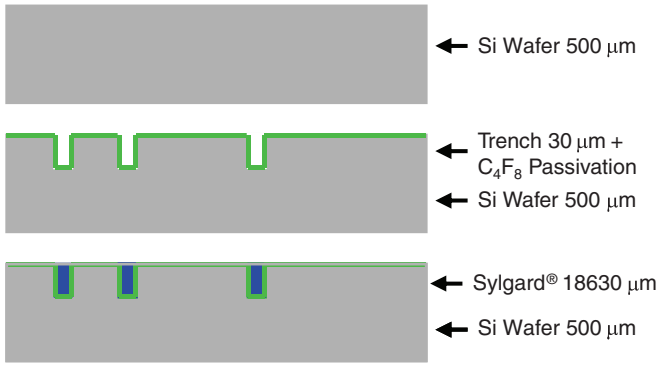

Figure 6. Process for molding microrubber bands.

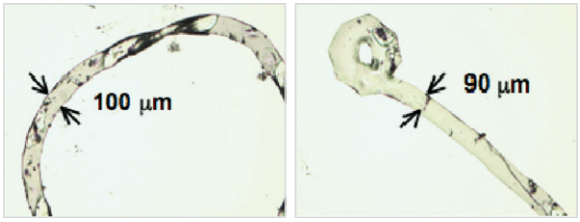

Figure 7. Molded microrubber bands. These show significantly cleaner edges and may be fabricated into new shapes such as the barbell at right.

similar to that demonstrated in [19]. However, in this process, C_4F_8 gas is used at 600 W for 3 min to passivate the mold. Thinned and vacuumed Sylgard® 186 silicone is then poured into the mold and placed into the vacuum for an additional 30 min. Finally, the excess silicone is scraped off with a razor blade and the silicone remaining in the trenches is cured at 100 °C for 45 min. After curing, it is possible to simply remove the rubber with tweezers (figure 7). Three different thicknesses were fabricated: 20 μm, 30 μm and 40 μm.

3.3. Assembly

After both silicon microstructures and microrubber bands have been fabricated, fine point tweezers are used to assemble rubber bands onto silicon hooks under a stereo inspection microscope (figure 1). Post-process assembly supports the use of polymers not compatible with processing steps, and without

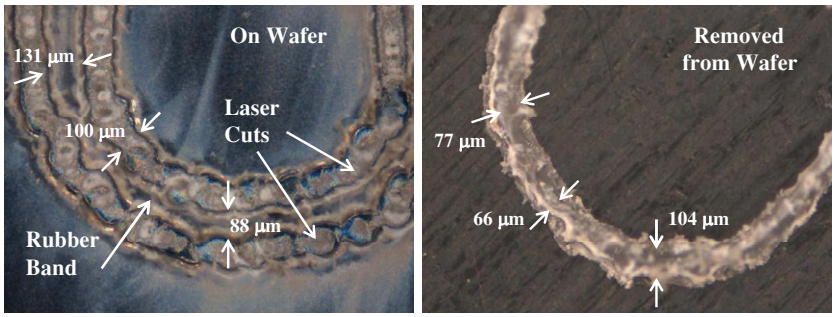

Figure 5. Laser cut microrubber bands. At left, the laser cuts can be seen while the microrubber band is still on the wafer and at right, the microrubber band has been removed from the wafer.

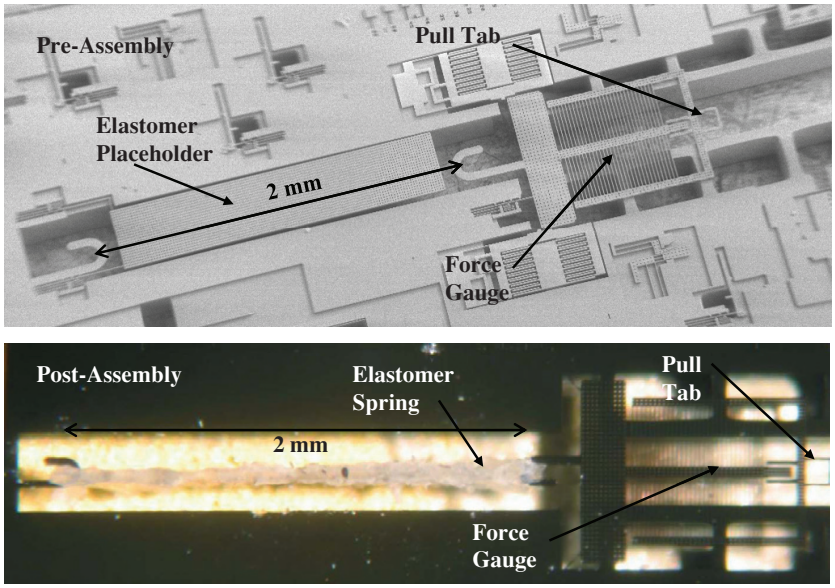

Figure 8. Force gauge test structure for characterizing microrubber bands.

the need for complex bonding and alignment in a clean room. Since at least one of the hooks is generally connected to a moving part, it is critical to assembly success that the moving part be tethered during assembly. These tethers need to be strong enough to resist forces encountered during assembly from tweezers or silicone, yet simple to break after assembly was completed. A tether design similar to that shown in [17] was used and found to be suitable for this application. Assembly yield has been approximately 80% with failures usually resulting from sudden hand movements, although this number has improved substantially with practice.

4. Elastomer characterization

Once fabricated and assembled, the microrubber bands were characterized on their utility for energy storage and release. A force gauge was fabricated in the SOI process to measure the force–distance curves and energy storage efficiency of the silicone microrubber bands (figure 8). This force gauge was designed to withstand forces greater than 10 mN and measure the applied force with a resolution of 200 μN. The fabricated microrubber bands were assembled onto the force gauge pre-strained to insure they were taut and could not slip off the hooks. After breaking the tether holding the force gauge in place, a probe tip was used to pull the force gauge and rubber band while force and distance measurements were recorded. Data were collected for both the laser cut rubber bands and molded rubber bands.

Laser cut rubber bands approximately 75 μm wide, 50 μm thick and 1.1 mm in diameter were assembled with an approximate pre-strain of 16% and tested first. Results from two of the trials for laser cut microrubber bands are shown in figure 9. In trial 1, the elastomer band was stretched 165% to store 7.2 μJ of energy and 81% of that energy was recovered upon slowly releasing the spring. In trial 2, the elastomer band was stretched 183% and stored 8.2 μJ of energy with an efficiency of 85%. Other trials showed up to 11 μJ stored and 93% recovered energy efficiency.

The same experiment was performed with molded rubber bands of approximately the same size 100 μm wide, 30 μm thick and 1.2 mm in diameter. These rubber bands were measured to have a pre-strain of approximately 11% and results from two trials are shown in figure 10. In trial 1, the molded microrubber band was stretched 200% to store 10.4 μJ of energy and 92% of that energy was recovered upon slowly releasing the spring. In trial 2, the rubber band was stretched to over 220% strain. In this trial, 19.4 μJ of energy was stored and 16.5 μJ was released for an efficiency of 85%.

The four trials outlined above resulted in calculated spring constants that differ substantially. Both of the spring constants using the laser cut rubber bands were approximately 2.1 N m^{-1}. However, for the molded rubber bands, the calculated spring constant for the first trial was 1.6 N m^{-1} while the second trial was calculated at 2.5 N m^{-1} even though both rubber bands were fabricated in the same mold. It is assumed that the microrubber band fabricated in trial 1 was damaged when removed from the mold resulting in the significantly lower spring constant. The same assumption holds true for the laser cut rubber bands, which were obviously damaged by the laser. Therefore, an approximate Young's modulus for Sylgard® 186 may be calculated from the fourth trial using the equation

$$E = \frac{k}{2} \cdot \frac{L}{A}, \tag{3}$$

where k is the calculated spring constant (2.5 N m^{-1}), L is the length of the microrubber band (1.8 mm) and A is the cross-sectional area of the band (3000 μm^2). This calculation results in Young's modulus of 750 kPa which is very similar to the 700 kPa calculated in [18].

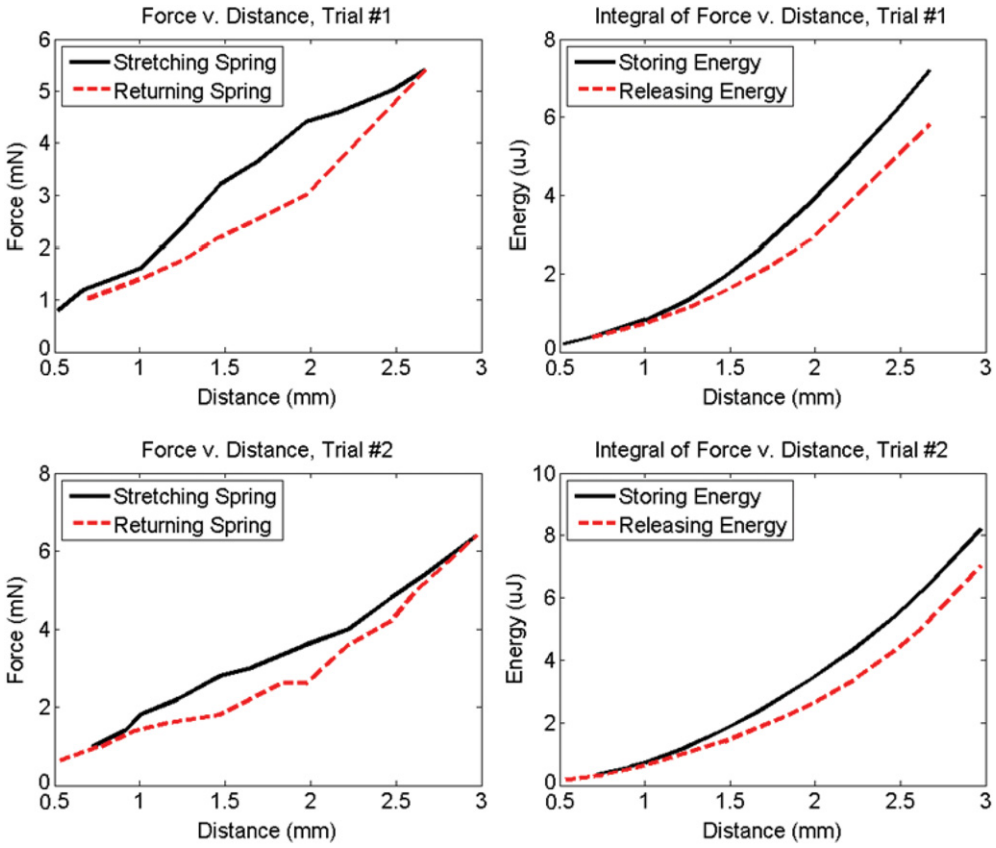

Figure 9. Force–distance curves for laser cut Sylgard® 186.

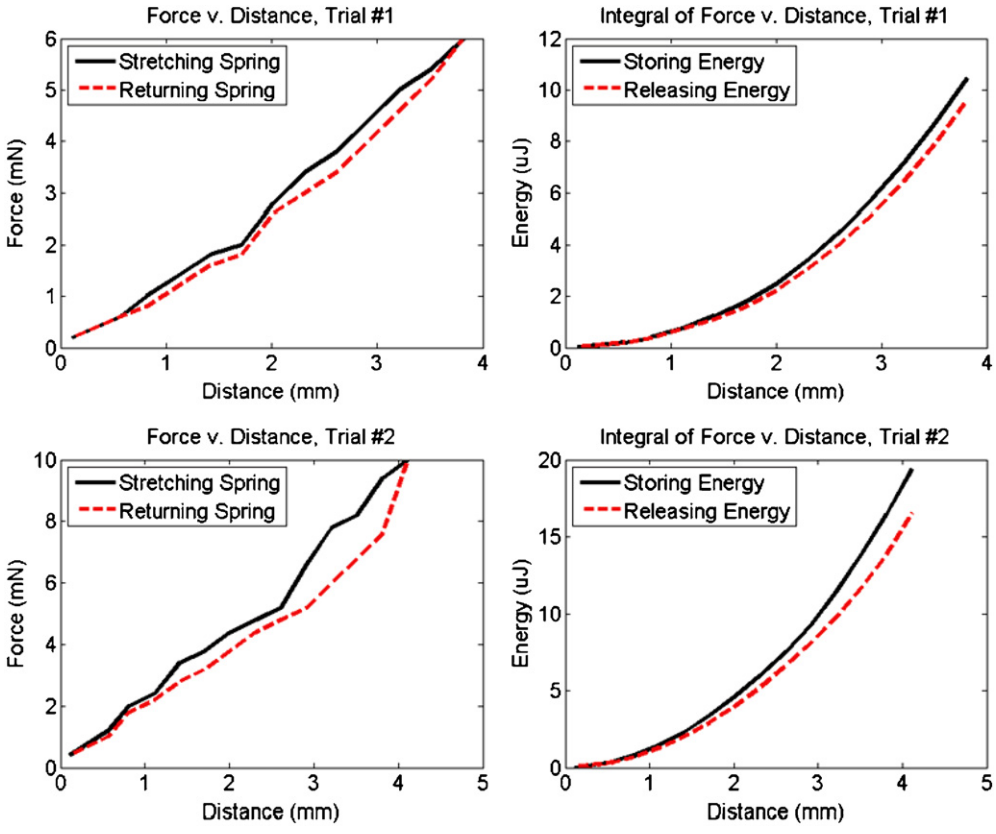

Figure 10. Force–distance curves for molded Sylgard® 186.

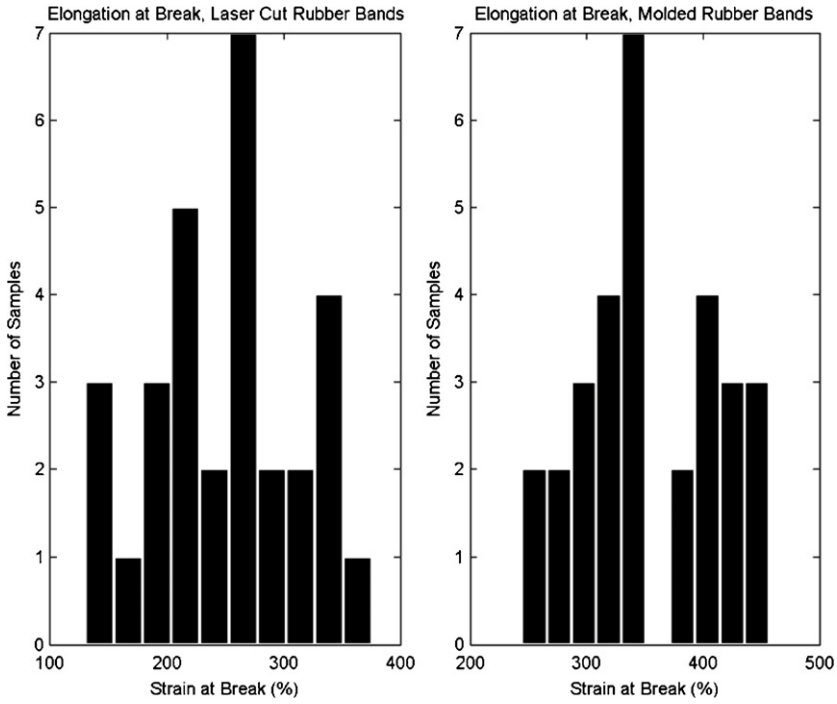

Figure 11. Histograms of elongation at break tests. The laser cut microrubber bands break at a significantly lower strain than the molded microrubber bands.

4.1. Elongation at break

In addition to measuring recovered energy efficiency and Young's modulus of the microrubber bands, it is also important to know when they break. The failure strain of these bands was measured by stretching the rubber bands with tweezers until they snapped (figure 11). For the laser cut silicone, a mean failure strain was measured at approximately 250% over 30 trials with a standard deviation of 60%. The molded silicone fared significantly better with a mean failure strain of 350% over 30 trials and a standard deviation of 60%. The similar standard deviation in the molded rubber bands is probably due to the current method of removing the rubber bands from the mold with tweezers, which slightly damages them. However, they still demonstrate significantly higher performance than the rubber bands that were laser cut.

4.2. Micro rubber band longevity

In order to measure the effect that time had on the durability of the rubber bands, an elongation-at-break test was performed at regular time intervals. Tests were done on 20 laser cut microrubber bands at 0 weeks (directly after laser cutting), 2 weeks and 4 weeks. This test was done on rubber bands made of Sylgard® 186 of three different drawn widths (200 μm, 300 μm, 400 μm). During the first 2 weeks there was a noticeable decrease in the length of elongation before break. The 300 μm wide bands decreased by 10%. However, in the 2 weeks after that, the data stayed roughly the same with average fluctuations +/− 2%. This data can be seen in figure 12.

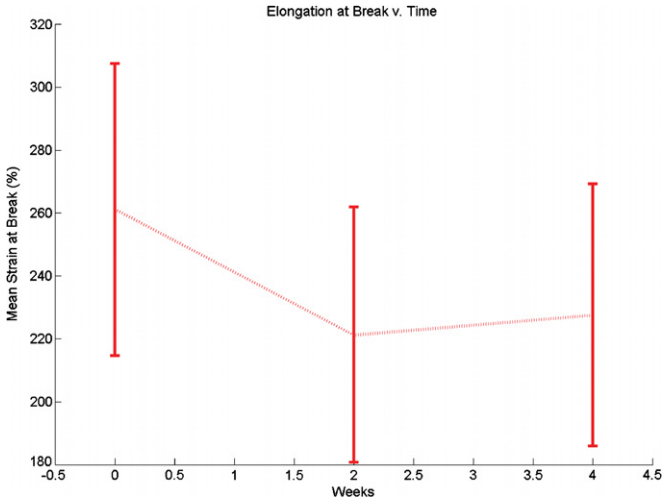

Figure 12. Elongation at break over time. After the first 2 weeks, the elongation at break mean stayed within 2% of the previous weeks value.

4.3. Quick release

To explore the effects of quickly releasing the stored energy as will be required in a high power application like jumping microrobots, a test structure was designed to shoot a projectile across a surface (figure 13). This test structure consists of a microrubber band attached to the body of the test structure on one side and a leg connected to a force gauge on the other end. In addition, electrostatic GCA clamps are used to hold the leg in place before release. These clamps are designed to be normally closed so that the clamps open by actuating away from the leg. The advantage of this method over electrostatically closing normally open clamps is twofold.

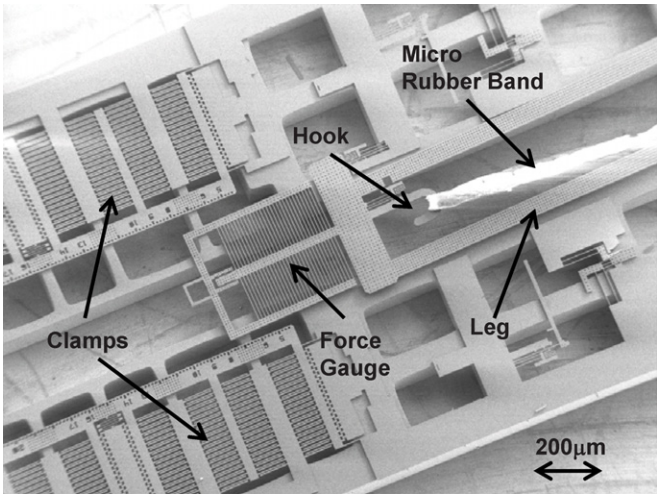

Figure 13. Quick release test structure with elastomer connected to leg which can be held before release with electrostatic clamps.

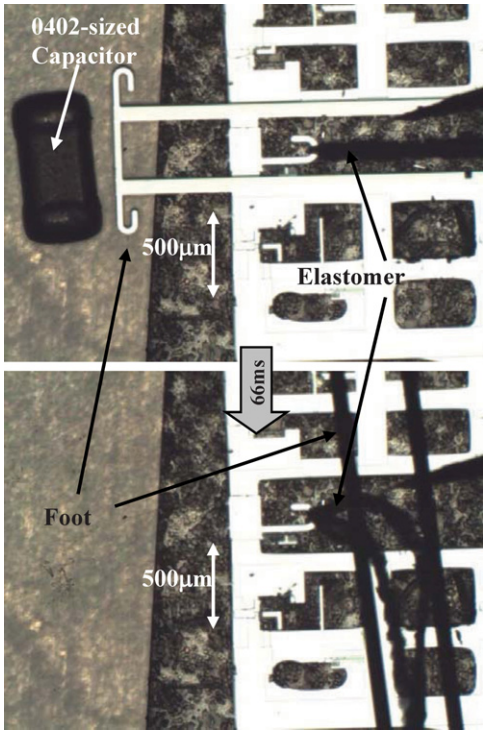

Figure 14. Quick release test structure shooting a surface mount capacitor. The top shows the frame captured directly before releasing the clamps and the bottom shows the frame directly afterwards. The camera captured the video at 15 fps.

Because the flexure force is linear with respect to displacement, the leg self-centers and equal force is provided on both sides of the leg. In addition, the test structure may also be moved and re-oriented while the clamps are held closed.

For testing, the test structure was held with double stick tape on a glass slide under a probe station and the leg was pulled back with a probe and clamped. A 0402-sized capacitor with a mass of approximately 0.6 mg was then maneuvered in front of the leg (figure 14). Finally, the clamps were actuated to release the leg. While the total energy released is not quantified here, video showed that the leg released its energy in less than a single video frame (66 ms) and the leg propelled the resistor 1.5 cm along the glass slide. The primary failure mechanism was the leg popping out of plane as seen in the bottom half of figure 14. In the future, assembled staples over the leg as demonstrated in [9] should be able to fix this problem by preventing the leg from moving vertically out of plane.

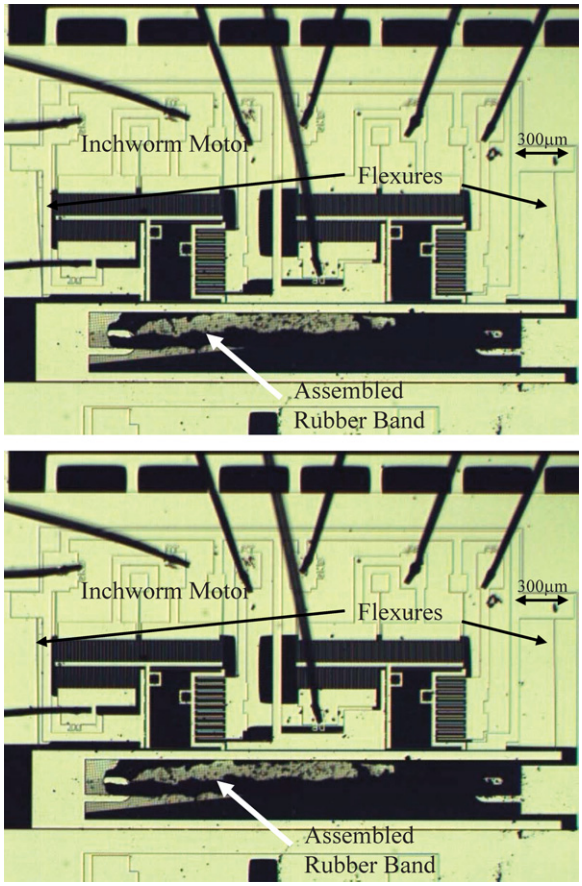

Figure 15. Electrostatic inchworm motor pulling a microrubber band. The top frame shows the pre-loaded microrubber band and the bottom frame shows the inchworm motor after pulling the microrubber band 30 μm to store 4.9 nJ.

5. Integrated system results

Finally, a fully integrated micromechanical energy storage system was designed and tested by adding an actuator to load the microrubber band before releasing it. A laser cut silicone microrubber band was assembled pre-strained into a small electrostatic inchworm motor. In this case, the inchworm motor provides yet another advantage by using the clutch actuators as clamps to quickly release the shuttle connected to the rubber band (figure 15). For this test, the inchworm motor was actuated with an off-board controller at 90 V for approximately 225 μN of force and displaced 30 μm, at which point the motor's gear teeth began to slip.

To calculate the energy stored by the inchworm motor, it was first necessary to determine the amount of energy stored while assembling the microrubber band. A load force of 100 μN from pre-straining was estimated by assembling a similarly fabricated microrubber band into a force gauge

elsewhere on the chip. Pre-loading shifts the force–distance curve above the origin. For this test, approximately 3 nJ was stored due to pre-loading during assembly.

The energy stored by the inchworm motor was calculated by assuming that the maximum force of 225 μN was used towards loading the microrubber band. Therefore, it was estimated that the inchworm stored an additional 1.9 nJ of energy before slipping for a total of 4.9 nJ stored and quickly released. It is important to note that the motor and clamping mechanism make this system reusable so that energy can be stored, quickly released, stored again, and so on. Inchworm motors designed more aggressively for larger forces and displacements will push this stored energy significantly higher to the micro-Joule range.

6. Conclusions and future work

This paper has presented the design of a reusable micromechanical energy storage/quick release system as well as a process with flexibility in integrating elastomer materials as springs into silicon microstructures. Two separate methods for fabricating elastomer springs were presented, both of which have advantages. Laser cutting silicone is a quick, fab-less way of creating springs but suffers from poor yield and lower quality microrubber bands with less design flexibility. Molding allows substantially greater flexibility in spring design and produces high quality microrubber bands, but requires a clean room and extra time for fabricating the mold. While only Sylgard® 186 has been characterized thus far, testing new types of elastomers including other silicones and latex offers excellent opportunities for future work.

A fully integrated micromechanical energy storage system that stored and quickly released 4.9 nJ was also demonstrated. While almost 20 μJ was stored in the microrubber band using a probe tip during characterization, the next step toward building an autonomous jumping microrobot will be designing an actuator that can do the same. Assuming a 10 mg mass similar to the autonomous microrobot designed in [1], 20 μJ would result in a jumping height of 20 cm. Finally, a more precise characterization of the efficiency resulting from quickly releasing the stored energy as shown in the projectile test will be important for the final goal of an autonomous jumping microrobot.

Acknowledgments

Special thanks to Professor Ron Fearing and the members of his laboratory for providing instruction on and use of the VersaLaser® laser cutter. In addition, the authors would like to thank the staff and members of the UC Berkeley Microfabrication Laboratory for their assistance.

References

[1] Bergbreiter S and Pister K S J 2007 Design of an autonomous jumping microrobot *IEEE Int. Conf. Robotics and Automation*

[2] Arora A, Hakim I, Baxter J, Rathnasingham R, Srinivasan R, Fletcher D A and Mitragotri S 2007 Needle-free delivery of macromolecules across the skin by nanoliter-volume pulsed microjets *Proc. Natl. Acad. Sci. USA* **104** pp 4255–60

[3] Rodgers M S, Allen J J, Meeks K D, Jensen B D and Miller S L 1999 A micromechanical high-density energy storage/rapid release system *SPIE Conf. on Micromachined Devices and Components V* vol 3876 pp 212–222

[4] Rose C and Wright G 2004 Inscribed matter as an energy-efficient means of communication with an extraterrestrial civilization *Nature* **431** 47–9

[5] Lotters J C, Olthuis W, Veltink P H and Bergveld P 1997 The mechanical properties of the rubber elastic polymer polydimethylsiloxane for sensor applications *J. Micromech. Microeng.* **7** 145–7

[6] Tung Yi-C and Kurabayashi K 2005 A single-layer pdms-on-silicon hybrid microactuator with multi-axis out-of-plane motion capabilities: Part 1. design and analysis *J. Microelectromech. Syst.* **14** 548–57

[7] Bennet-Clark H C 1976 Energy storage in jumping insects *The Insect Integument* (Amsterdam: Elsevier) pp 421–443

[8] Chong D Y R, Lee W E, Lim B K, Pang J H L and Low T H 2004 Mechanical characterization in failure strength of silicon dice *IEEE Thermal and Thermomechanical Phenomena in Electronic Systems* **vol 2** pp 203–10

[9] 6.777j/2.751j Material Property Database 2007 http://web.mit.edu/6.777/www/matprops/pdms.htm

[10] Vitek coatings—parylene coatings 2007 http://www.vitekres.com/vitekparylene.htm

[11] Mahadevan R, Mehregany M and Gabriel K J 1990 Application of electric microactuators to silicon micromechanics *Sensors Actuators* A **A21–A23** 219–25

[12] Howard M J (ed) 1977 *Elastomeric Materials* (San Diego, CA: The International Plastics Selector)

[13] Li Y and Unsworth J 1993 Dynamic mechanical behaviours of epoxy insulating composites *Electrical Electronics Insulation Conf.* pp 7–11

[14] Yeh R, Hollar S and Pister K S J 2002 Single mask, large force, and large displacement electrostatic linear inchworm motors *J. Microelectromech. Syst.* **11** 330–6

[15] Suzuki Y and Tai Y-C 2006 Micromachined high-aspect-ratio parylene spring and its application to low-frequency accelerometers *J. Microelectromech. Syst.* **15** 1364–70

[16] Engel J M, Chen J, Liu C and Bullen D 2006 Polyurethane rubber all-polymer artificial hair cell sensor *J. Microelectromech. Syst.* **15** 729–36

[17] Last M, Venkatraman S and Pister K S J 2005 Out of plane motion of assembled microstructures using single-mask soi process *Transducers* 684–7

[18] Pelrine R, Kornbluh R, Joseph J, Heydt R, Pei Q and Chiba S 2000 High-field deformation of elastomeric dielectrics for actuators *Mater. Sci. Eng.* C 89–100

[19] Gao J X, Yeo L P, Chan-Park M B, Miao J M, Yan Y H, Sun J B, Lam Y C and Yue C Y 2006 Antistick postpassivation of high-aspect ratio silicon molds fabricated by deep-reactive ion etching *J. Microelectromech. Syst.* **15** 84–93